Corrosion Science 53 (2011) 637–644

Contents lists available at ScienceDirect

Corrosion Science

journal homepage: www.elsevier.com/locate/corsci

Correlation between critical pitting temperature and degree of sensitisation on alloy 2205 duplex stainless steel

N. Ebrahimi [a], M. Momeni [a,*], M.H. Moayed [a], A. Davoodi [b]

[a] Metallurgical and Materials Engineering Department, Ferdowsi University of Mashhad, Mashhad 91775-1111, Iran
[b] Materials Engineering Department, Sabzevar Tarbiat Moallem University, Sabzevar 391, Iran

ARTICLE INFO

Article history:
Received 12 June 2010
Accepted 17 October 2010
Available online 25 October 2010

Keywords:
A. Stainless steel
B. Polarisation
C. Pitting corrosion
C. Intergranular corrosion
C. Passivity

ABSTRACT

In this study effect of different ageing conditions on intergranular corrosion, pitting corrosion and relation between critical pitting temperature (CPT) and degree of sensitisation (DOS) was investigated by potentiostatic polarisation and double loop-EPR methods. The results showed by increasing sensitisation time, DOS increased and measured CPT value decreased. In addition the values of DOS and CPT of specimens aged at 650 °C showed almost liner relation while this correlation was diminished for the specimens aged at 800 °C. The results may be attributed to the further formation of precipitates on specimens aged at temperature of 800 °C.

1. Introduction

Duplex stainless steels (DSS) containing two-phase austenite–ferrite microstructures are of interest for various applications such as petroleum, gas refineries and marine environments particularly due to their permutation corrosion and mechanical properties [1–8]. Chromium (Cr) and molybdenum (Mo) enrich ferrite, while nitrogen (N) and nickel (Ni) are mainly found in austenite [9]. Because of the high content of alloying elements, the duplex stainless steels show complex phase transformation and precipitation behaviour [10]. The best general properties are obtained with approximately equal amounts of austenite and ferrite and the absence of third phases such as σ and χ [6,11]. However, due to high chromium and molybdenum contents and their high diffusion rate in ferrite, DSS are prone to form some unwanted secondary phases during exposure to elevated temperatures between 400 and 1000 °C [12,13].

These precipitation processes of secondary phases in DSS are classified in two clearly distinct temperature intervals [14,15]. The higher interval is between 550 and 1000 °C, where phases such as nitrides, carbides, σ and χ are clearly separated from each other, [16–22]. The lower interval is in temperature range of 400–500 °C, where Cr-rich α′ phase precipitates due to spinodal decomposition of the ferrite phase [23–25]. These phases can be formed from ferrite when the DSS is welded or hot worked [5]. Among all precipitate types, sigma phase is the major concern due to its detrimental influence on both mechanical properties and corrosion behaviour [17,26,27]. Sigma is an intermetallic phase enriched by Cr and Mo [10,28]. Due to its high Cr and Mo content, the precipitation of sigma phase depletes the surrounding regions of Cr and Mo, leading to a decrease in corrosion resistance of duplex stainless steel [29–31]. In this study effect of different sensitising treatments on corrosion behaviour of DSS2205 and dependence of critical pitting temperature (CPT) on degree of sensitisation (DOS) of this alloy has been investigated.

2. Experimental methods

The chemical composition analysis of alloy in weight percent was 0.03% C, 0.97% Mn, 0.022% P, 0.0007% S, 0.74% Si, 21.61% Cr, 5.31% Ni, 3.07% Mo, 0.16% Cu, 0.136% V, 0.064% W, 0.01% Ti, 0.15% N and Fe balance, which is in agreement with the AISI 2205 (UNS S31803). For studying the relation between critical pitting temperature (CPT) and degree of sensitisation (DOS), the alloy was aged at 650 and 800 °C for 10, 60 and 300 min. Specimens were held in an air atmosphere furnace with temperatures of 650 and 800 °C for different selected times, followed by water quench to produce different degrees of sensitisation. The alloy microstructure was characterised by optical microscopic (OP) examination. All specimens were polished to 0.05 μm alumina slurry. The etching was done at 2.5 V DC for 10 s in oxalic acid followed by 1.5 V DC for 10 s in 10 M KOH while specimen was anode and a platinum wire was used as cathode [32]. Then, the specimens were rinsed by distilled water, washed by methanol and dried by hot air. To investigate the microstructure by scanning electron

* Corresponding author. Tel./fax: +98 5118763305.
E-mail address: mojtaba.momeni@stu-mail.um.ac.ir (M. Momeni).

0010-938X/$ - see front matter © 2010 Elsevier Ltd. All rights reserved.
doi:10.1016/j.corsci.2010.10.009

microscope (SEM model Philips XL 20), specimens were etched in 10% oxalic acid according to the ASTM A-262A [33]. In addition, the presence of different phases were analysed by X-ray diffraction (XRD) with Cu Kα radiation.

DOS values of specimens were measured by double loop electrochemical potentiodynamic reactivation (DL-EPR) method in 0.3 M HCl + 0.002 M $Na_2S_2O_3$ solution and scan rate of 100 mV/min [34]. The specimens were polarised from 50 mV below OCP to anodic region and scanning direction was reversed from 0 mV vs. SCE toward OCP. DOS values were measured using the ratio of maximum current density of reactivation to maximum current density of activation according to the following equation.

$$\mathrm{DOS}\% = \frac{i_r}{i_a} \times 100 (1) \quad (1)$$

The CPT values were measured in 0.1 M NaCl solution employing potentiostatic polarisation method. The specimens were polarised at anodic potential +750 mV with respect to open circuit potential and temperature was increased by a rate of 0.6 °C/min. The CPT value was considered as the temperature which current density reached 100 μA/cm^2 [35]. Temperature was controlled using water bath.

Saturated calomel electrode (SCE) and platinum wire were used as reference and counter electrodes, respectively. Electrochemical tests were conceded by means of Gill AC automated potentiostat (ACM Instruments). Before each polarisation test, open circuit potential (OCP) was obtained for 15 min. Each experiment was repeated for three times to ensure their reproducibility.

3. Results and discussion

3.1. Microstructural analysis

Fig. 1 shows microstructure of DSS2205 alloy in different heat treatment times at 650 and 800 °C. Darker phases represent ferrite while brighter phases are austenite. The as-received specimen did not show any dissolved precipitates at grain boundaries. In other word, this specimen was not sensitised. Although it was reported elsewhere [36] that by 10 min ageing of DSS2205 in temperature range of 600–700 °C chromium nitrides (Cr_2N) could precipitate at ferrite–ferrite boundaries, in microstructure of 10 min aged specimen at 650 °C no dissolved precipitates at grain boundaries could be observed. Similar condition can be seen in microstructure of 10 min sensitised specimen at 800 °C.

Results of 60 min sensitised specimen at 650 °C was similar to previous ageing time in this temperature indicating that in this treatment temperature, no remarkable precipitate could form at grain boundaries. However it can be considered that some precipitations were nucleated at grain boundaries and the existing precipitates were coarsened by increasing the ageing time from 10 to 60 min. The 60 min sensitised specimen at 800 °C shows dissolved precipitates at grain boundaries. Which means, due to ageing of the specimen at 800 °C some precipitates were formed at grain boundaries and these precipitates were dissolved in etching process. Since 800 °C is the critical temperature in time–temperature–precipitation (TTP) diagram of DSS2205 alloy [36], many types of precipitates can be formed at this temperature. It was reported that after 60 min ageing of DSS2205 at 800 °C sigma phases are formed in boundaries of ferrite and austenite and the volume fraction of chi phase is negligible in compression with sigma phase [36]. It was also reported that in this temperature Cr_2N precipitates could be found in boundaries of ferrite and austenite and also ferrite/ferrite boundaries by increase in time [37]. The precipitates in 300 min sensitised specimens at both ageing temperatures were completely clear.

By looking to the microstructure of all sensitised specimens, it is obvious that the precipitate growth direction is in ferrite phase. In other word, the precipitates are more likely to grow in ferrite rather than austenite. This can be attributed to the fact that chromium and molybdenum content of ferrite is higher than austenite and the diffusion coefficient of chromium in ferrite is almost 10 times higher than austenite [38]. Therefore, the precipitates like chromium carbides, sigma phase, chi, etc. grow into the ferrite phase. On the other hand higher value and diffusion coefficient of these elements in ferrite, leads to two different chromium (and molybdenum) depleted profile in austenite and ferrite grains. The profile in austenite is narrow and deep while it is wide and shallow in ferrite [38]. As a result, as it can be seen in microstructure of sensitised specimens, especially 300 min sensitised ones, it seems that the precipitates were formed in ferrite phase. On the other hand, it was also reported that by increasing the ageing time and formation of sigma phase, chromium and molybdenum content of ferrite decreases and partially Ni content increases. As a result ferrite phase undergoes decomposing and secondary austenite and sigma phase may be formed [9,35,38]. Furthermore, in all sensitised specimens chromium carbides can be found as well as other intermetallic precipitates [39].

Fig. 2 shows changes in volume fraction of phases by changing ageing condition (analysis of volume fractions was perform by Clemex software). The results demonstrate that austenite volume fraction is almost constant and it is in the range of 46–56% which is in agreement by equilibrium volume fraction of DSS2205. On the other hand as it was explained above, precipitates are more likely to grow in ferrite phase. As a result ferrite volume fraction decrease from 51% at non-sensitised specimen to 21% at 300 min sensitised specimen at 800 °C. Although various types of precipitates are formed in microstructure due to the different heat treatment conditions, in this study, to investigate the precipitates volume fraction by OP, volume fraction of all precipitates and their affected zone due to etching process is considered as precipitate volume fraction. It is obvious that by 300 min ageing at 800 °C, precipitate volume fraction increase to 36% while it is almost 10% at 60 min sensitised specimen at 800 °C and below 1% at 300 min sensitised specimen at 650 °C.

XRD results of as-received and 300 min sensitised specimens is shown in Fig. 3. The results demonstrate as-received specimen pattern contain only ferrite and austenite peaks. As it was mentioned above, precipitate fraction in 300 min sensitised specimen at 650 °C was low and as a result, no considerable precipitate was detected by XRD in this specimen. In the XRD results of 300 min sensitised specimen at 800 °C, some additional peaks were observed which are related to the sigma phase. As it was discussed above, different types of intermetallic phases could precipitate in this heat treatment, however, the most significant phase was sigma phase and consequently it was detected by XRD. In addition, by ageing the specimens, the intensity of ferrite and austenite phases was diminished due to their transformation to intermetallic precipitates.

3.2. Degree of sensitisation (DOS) measurement

Fig. 4 shows the SEM results of microstructure analysis after electrical etching by oxalic acid [34]. As it can be observed, as-received specimen showed almost no ditches in grain boundaries and this behaviour was repeated in microstructure of 10 and 60 min sensitised specimen at 650 °C. Although no considerable ditches in these two sensitised specimens were observed, grain boundary attack was increased by increasing the sensitisation time. The ditches in grain boundaries of 300 min sensitised specimen at 650 °C and all sensitised specimens at 800 °C are easily visible, indicating sensitisation occurrence. In addition it is completely clear that the grain boundary

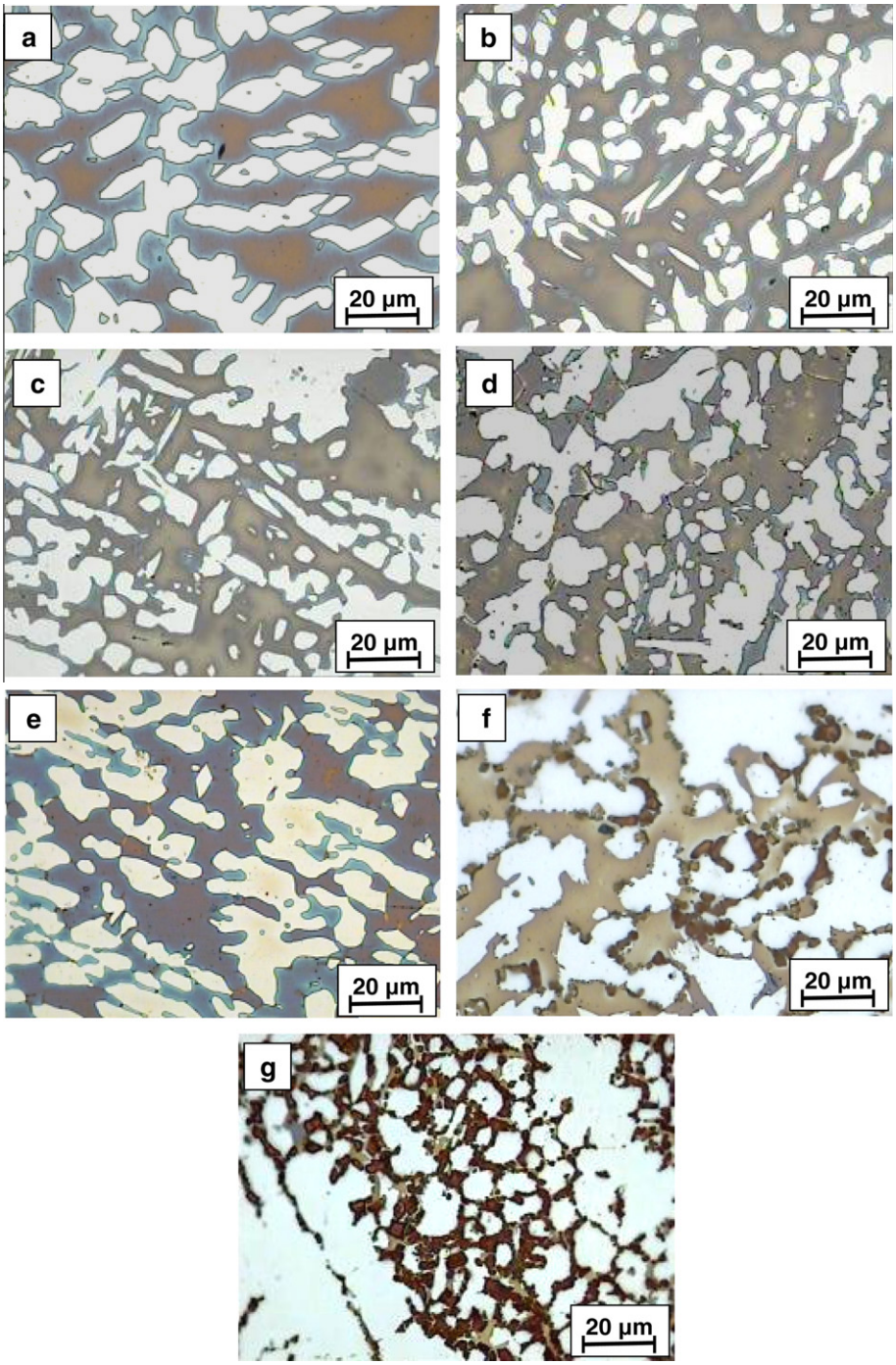

Fig. 1. Microstructure of DSS2205 (a) as-received, (b) 10 min sensitised at 650 °C, (c) 60 min sensitised at 650 °C, (d) 300 min sensitised at 650 °C, (e) 10 min sensitised at 800 °C, (f) 60 min sensitised at 800 °C and (g) 300 min sensitised at 800 °C.

attack in specimens sensitised at 800 °C was increased by increasing in ageing time. Interestingly, it is evident in a similar ageing time; the attack was higher in 800 °C than 650 °C. This increase in intergranular attack shows higher DOS of sensitised specimens at 800 °C. While microstructure analysis can detect sensitisation, it can not measure it.

Fig. 5 shows measured DOS value of different sensitised DSS2205 specimens at 650 and 800 °C. It can be seen that by increasing the sensitisation time, DOS value increase. This means that the depleted chromium width in vicinity of grain boundaries and especially in ferrite grains was increased. In other word by increasing the ageing time, susceptibility to intergranular corrosion was increased due to depletion of chromium. This phenomenon could be detected by SEM microstructure analysis after oxalic acid etching process. However, as it can be seen, value of DOS in non-sensitised specimen was almost 1.1 and by sensitising the specimen for 10 min this value increased to 4.52 and 6.62 at 650 and 800 °C, respectively. This indicates that by 10 min sensitising at 650 and 800 °C some precipitates which are mainly chromium nitrides (Cr_2N) [36] are formed in grain boundaries and as a result a region witch its chromium value is lower than inside the grain can be found in vicinity of grain boundaries. Therefore

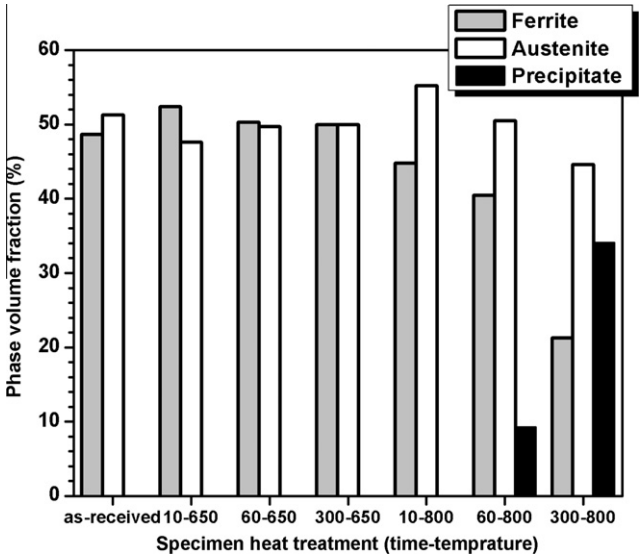

Fig. 2. Effect of different ageing condition on volume fraction of different phases of DSS2205.

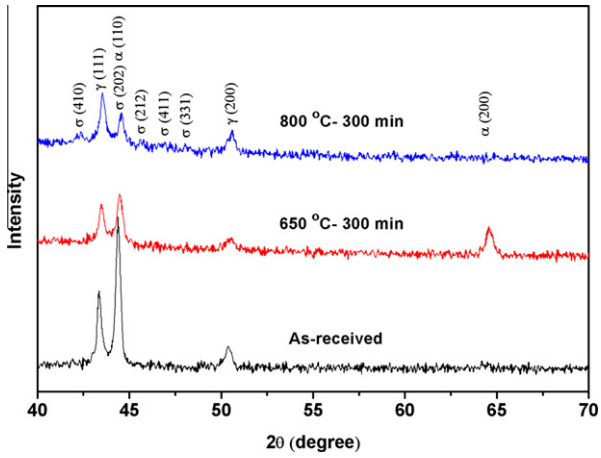

Fig. 3. XRD results of DSS2205 as-received, 300 min sensitised at 650 °C and 300 min sensitised at 800 °C.

passivity of chromium depleted region deteriorates and this week passivity, breaks down in reactivation state of DL-EPR. Considering values of DOS in the different sensitisation temperatures, it is obvious that higher sensitisation temperature gives higher value of DOS which confirms SEM results. This is due to the fact that in higher temperatures diffusion coefficient of chromium increases and while precipitation growth is controlled by diffusion of chromium rather than nitrogen, the higher value of diffusion coefficient of chromium promotes nucleation and growth of chromium nitrides at 800 °C more than 650 °C. By increasing sensitisation time from 10 to 60 min DOS value increased from 6.62 to 47.61 and 4.52 to 7.51 at 800 and 650 °C, respectively. As it can be observed, at 650 °C DOS value did no change considerably, while there is a significant increase in DOS value at 800 °C, as it was shown in SEM results, This jump in DOS value can be attributed to increasing in precipitates number and coarsening of the existed precipitates, leading to growing the chromium depleted regions and increasing their width. For instance, it is reported that by increasing ageing time form 10 to 60 min at 850 °C, the fraction of sigma phase in DSS2205 increases approximately from 1% to 7% [39] which is in agreement with the 9% precipitate phase reported in this study. As a result in reactivation stage of EPR test higher value of charge was created due to passivity break down. It was demonstrated previously [40] that the molybdenum element has great effect on passivity and increasing in molybdenum content decreases passive current density. As a consequence in 60 min sensitised specimen, by increasing sigma phase fraction and increasing the width of molybdenum depleted regions, passivity of depleted regions breaks down more easily. By increasing in ageing time at 650 °C, precipitate volume fraction did not change significantly. This indicates, between 10 and 60 min ageing periods at 650 °C passivity of grain boundary regions did not deteriorate in comparison with ageing at 800 °C.

The value of DOS in 300 min sensitised specimen increased to 25.74 and 54 for 650 and 800 °C, respectively. As it can be seen, DOS value for 650 °C increases significantly from 7.5 to 25.74 while there is no considerable change in DOS value of 300 min sensitised specimen at 800 °C in compression with 60 min sensitised specimen. Although sensitisation time increased from 60 to 300 min at 800 °C and microstructure analysis showed that this specimen was completely sensitised and volume fraction of precipitate phase increased to 36%, value of DOS was not increased significantly. This is due to the fact that, at high temperature and long ageing time, chromium and molybdenum diffuse from inside the grains to the depleted regions and minimum value of chromium in sensitised regions increase. As a result the passivity characteristic of depleted regions improves. On the other hand the value of DOS increased significantly by ageing the specimen at 650 °C for 300 min. This increase in DOS value shows increase in depleted region width. SEM micrographs confirm this observation that the most significant change in intergranular attack from 60 to 300 min was observed at 650 °C. However, DOS value of 300 min sensitised specimen at 650 °C was still lower than the specimens sensitised at 800 °C for 60 and 300 min.

3.3. Effect of ageing on critical pitting temperature

Fig. 6 shows a typical current vs. time curve for different sensitised DSS2205 specimens at 650 and 800 °C obtained from the CPT measurement test. It is evident that the current density was increased gradually by increasing temperature and the CPT was considered as the temperature in which current density reached 100 μA/cm^2 [35]. Considering Fig. 6 it can be found that the current density during the initial heating shows a value of lower than l0 μA/cm^2, indicating that the specimens were protected by the passive film. With increasing the solution temperature, some metastable current transients with different sizes were observed below the CPT, which was related to a film breakdown process occurring in a metastable pit [41–44]. Since below CPT the metastable pit cannot grow to stable pit and repassivates, the length of this type of pit was usually lower than 20 μA/cm^2 [36]. As the solution temperature increased more than the CPT, the current density increased abruptly due to the occurrence of stable pits. The CPT value of the as-received specimen was 60 °C; see Fig. 7. After 10 min ageing at 650 °C, the CPT of specimen did not change significantly and decreased to 56 °C. This was because Cr-rich precipitates could not completely precipitate in such a short time. However, the CPT of 10 min ageing specimen at 800 °C decreased to the value of 47 °C. This remarkable 13 °C decrease was due to the precipitation of Cr_2N at the ferrite/ferrite sub-grain boundaries. It was reported elsewhere that the content of chromium in Cr_2N reaches up to 94.3 wt.% [36]. Accordingly, such grain boundary Cr_2N precipitates were likely to cause chromium depleted zones and also accommodated substantial amounts of nitrogen, resulting in great decrease in CPT. As the ageing time increased further to 60 min, the CPT of aged specimens dropped to the 56 and 33 °C for ageing at 650 and 800 °C, respectively. It is clear that by

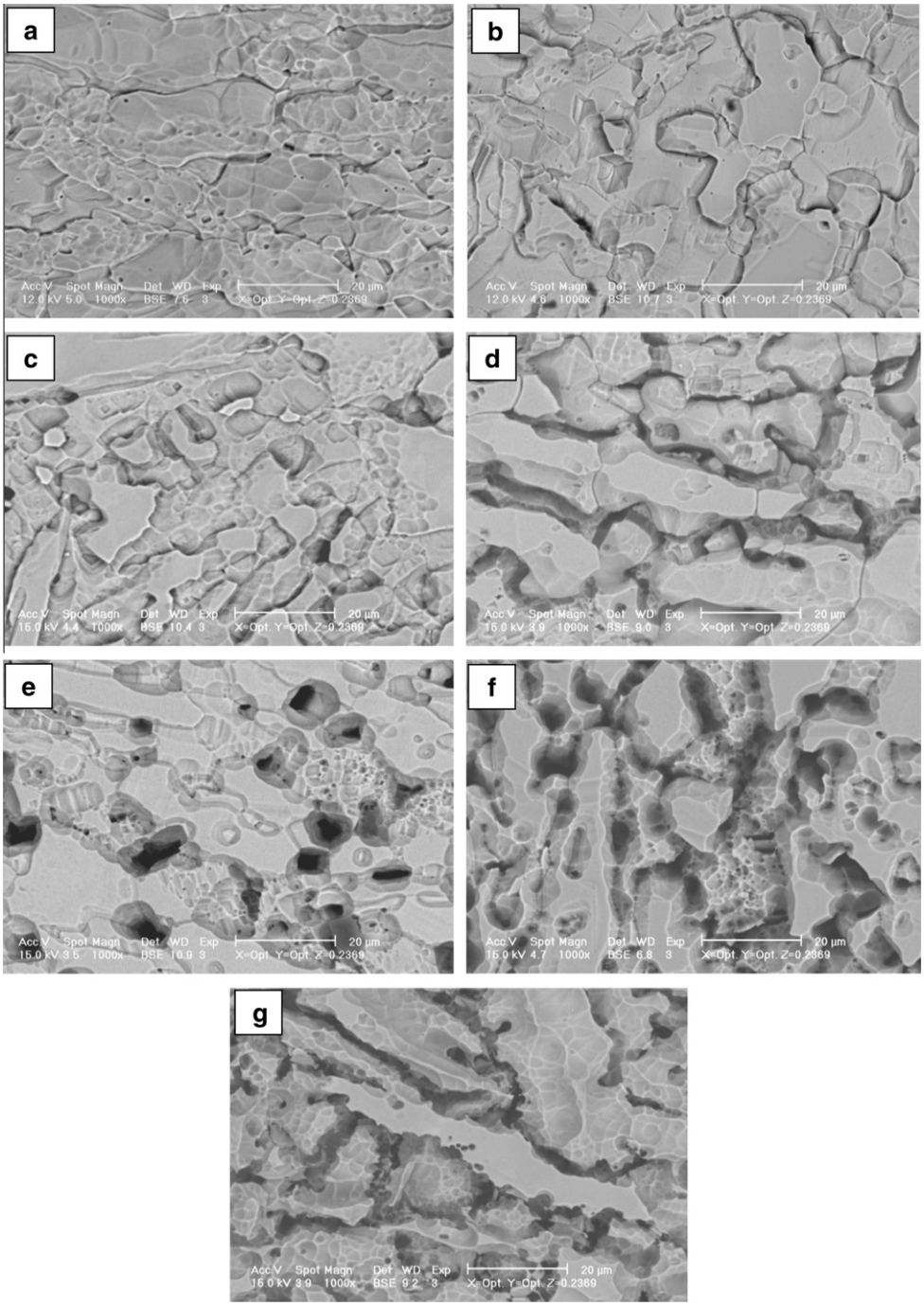

Fig. 4. SEM microstructure analysis of DSS2205 (a) as-received, (b) sensitised 10 min at 650 °C, (c) 60 min at 650 °C, (d) 300 min 650 °C, (e) 10 min at 800 °C, (f) 60 min at 800 °C and (g) 300 min at 800 °C etched by oxalic acid.

increasing ageing time from 10 to 60 min, the decrease in CPT value for specimen aged at 800 °C is very higher than that of 650 °C, mainly owing to the precipitation of relative large volume fraction of σ phase. The chemical composition of σ phase was reported as following: 57.64 Fe–30.14 Cr–4.20 Ni–8.02 Mo [36]. During its formation, Cr and Mo diffused from the ferrite to the growing σ phase. Thus causing localized depletion areas in Cr and Mo around the σ phase. These areas contain lower concentration of Cr and Mo and due to having higher amount of Ni they became unstable and transformed into secondary austenite ($\gamma 2$) [45]. It should be noticed that χ phase coexisted with σ phase after ageing at 800 °C and although its volume fraction was quite small compared to that of σ phase, it degrade the pitting corrosion resistance.

By increasing the ageing time to 300 min, the CPT decreased. This decrease is attributed to the content of intermetallic precipitates which increase at both ageing temperatures. However, the decrease in CPT value was significant in sample which was sensitised 300 min at 800 °C and its CPT value dropped to the 7 °C, while the CPT value of similar sample aged at 650 was 44 °C. In other word, the 300 min sensitised specimen at 800 °C was susceptible to the pitting corrosion even at room temperature. Considering the microstructural analysis, it is clear that by 300 min ageing of specimen the volume

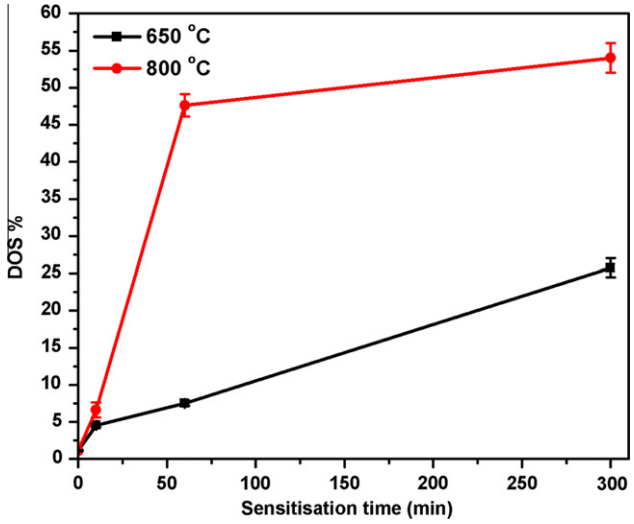

Fig. 5. DOS results of DSS2205 at different sensitisation conditions.

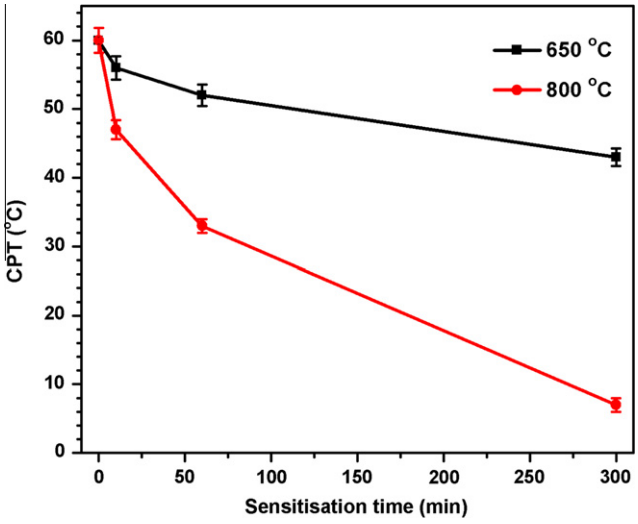

Fig. 7. CPT results for DSS2205 at different sensitisation conditions.

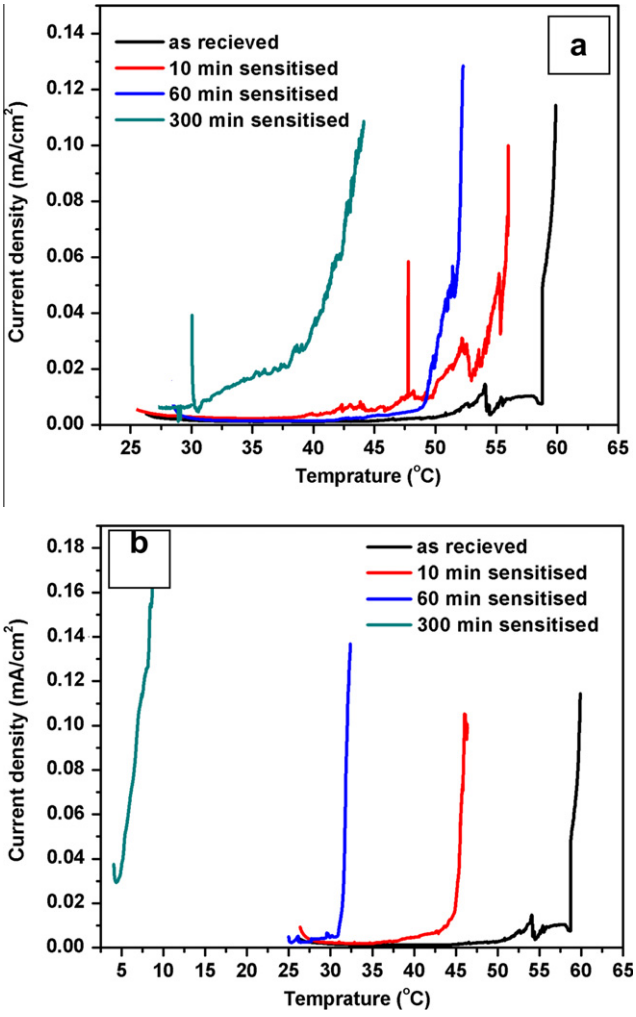

Fig. 6. Potentiostatic CPT measurements of different sensitised DSS2205 (a) 650° and (b) 800°.

fraction of ferrite phase decreased to almost 20%. This means that the specimen did not have duplex structure anymore. In other word, the beneficial effect of duplex structure could not be found in this specimen and as a result, it shows pitting corrosion at the ambient temperature like an austenitic stainless steel.

It can be realized from the above results that the presence of precipitates plays an important role in pitting initiation by deteriorating the passive film around the precipitates. Different types of precipitates formed during ageing at different temperatures can affect the pitting corrosion resistance [46]. In order to identify the preferential initiation sites of pitting; the specimen surface after pitting corrosion was examined by optical microscope. Fig. 8 shows the pits in microstructure of 300 min sensitised specimen at 800 °C. After pitting test the specimen surface was washed and cleaned ultrasonically by ethanol and etched by fry reagent. The microstructure was examined by optical microscopy. It can be realized that the pits are more likely to initiate from austenite phase. It was reported previously [36] that pitting resistance equivalent number (PREN) for austenite gives lower values than that of ferrite. As a consequence, the metastable pits are nucleated at the vicinity of precipitates in austenite.

3.4. Correlation between DOS and CPT of DSS2205

As it was demonstrated in previous sections, by increasing sensitisation time, DOS value increases and CPT decreases. Fig. 9

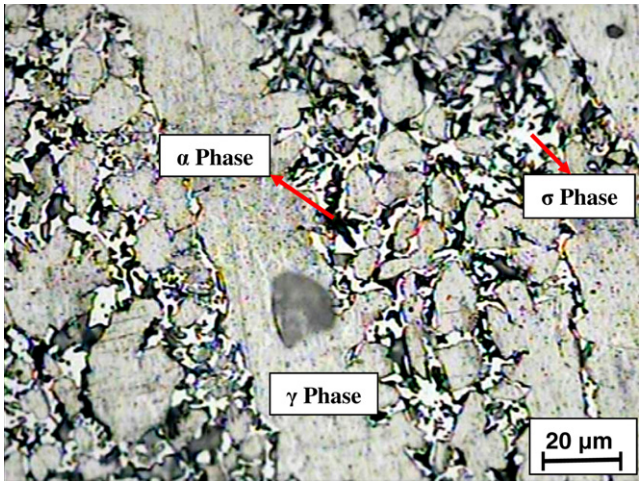

Fig. 8. Microstructural analysis of 300 min sensitised specimen at 800 °C after pitting corrosion test. The pit was formed on austenite phase.

shows the values of CPT as a function of DOS values for 650 and 800 °C. As it can be seen, the CPT and DOS of specimens sensitised at 650 °C show almost a liner relationship. Considering microstructural analysis, it is obvious that in specimens aged at 650 °C, no considerable precipitation could be found. In other word, microstructure of the specimens sensitised at 650 °C, shows typical duplex characteristic and the austenite–ferrite volume fraction is almost 50–50. By 10 min ageing the DSS2205 at 650 °C, CPT value decreased 4 °C while DOS increased 3% and further ageing to 60 min causes 4 °C decrease in CPT and 2% increase in DOS value. In other word, nucleating the precipitates at grain boundaries decreases CPT value and increases DOS. When specimen was aged for 300 min, both DOS and CPT values changed significantly and almost 10 °C decrease in CPT and 20% increase in DOS could be detected.

On the other hand this liner relation could not be observed in specimens aged at 800 °C. This phenomenon can be attributed to the change in microstructure of the specimens after ageing at 800 °C. While as-received and 10 min aged specimens showed duplex microstructure, the 60 min and 300 min sensitised specimens showed lower value of ferrite than that of duplex stainless steel, this is especially true for 300 min aged specimen. As a consequence, the linearity of DOS and CPT could not be observed in this temperature of ageing. By 10 min sensitising the specimen at 800 °C, CPT decreased about 13 °C while DOS increased only 6%. This can be attributed to the fact that in low ageing time, the precipitates were small and as a result their affected regions in matrix were small. However by increasing sensitisation time from 10 to 60 min, CPT decreases 14 °C and DOS increases from 6.62 to 48.61. As it was discussed in microstructure analysis section, by increasing the ageing time from 10 to 60 min the amount of precipitates increased and the existed precipitates were coarsened. Although increasing the precipitates number and their coarsening causes CPT value to decrease, their effect on passivity characteristic and DOS value was higher.

On the other hand by increasing sensitisation time from 60 to 300 min, as it was demonstrated above, the value of DOS increased from 48.61 to 54, while decrease in CPT value was significant and the 300 min sensitised specimen showed CPT value of 7 °C. The microstructure changes in ageing range of 60–300 min have higher influence on CPT in comparison with DOS. Although, by increasing the time chromium and molybdenum were diffused to grain boundaries and as a result the passivity characteristic was modified, the significant decrease in CPT and increase in DOS can be attributed to the significant increase in precipitate volume fraction.

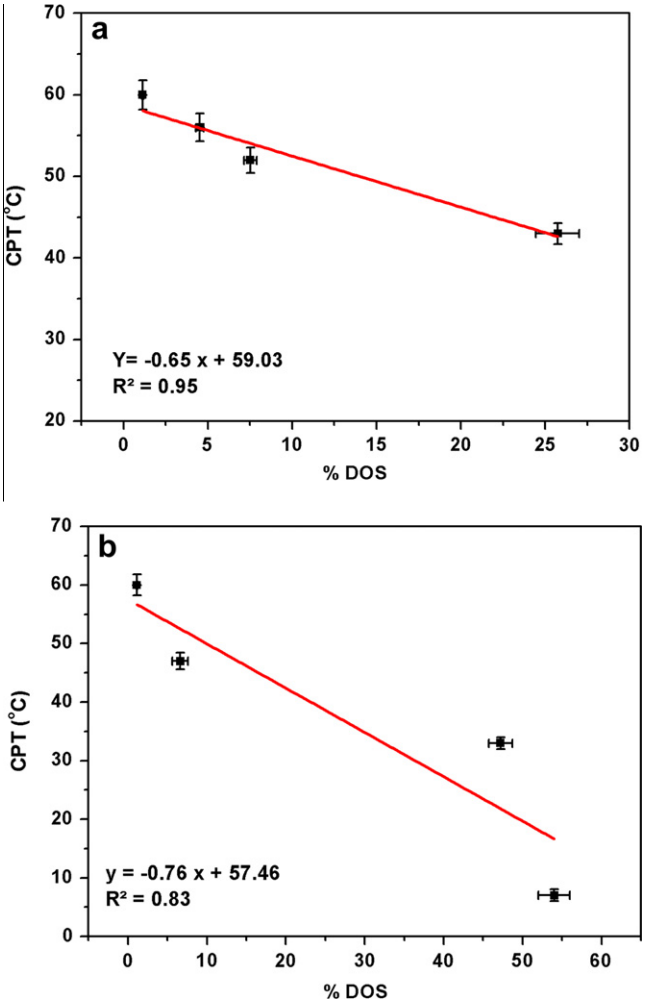

Fig. 9. Correlation between CPT and DOS values on DSS2205 (a) 650 °C and (b) 800 °C.

4. Conclusions

In this study effect of different ageing temperature and time on the pitting and intergranular corrosion of DSS2205 was investigated and following results were obtained:

1. The microstructural examination of DSS2205 showed by increasing ageing time at 800 °C, precipitates volume fraction increased and ferrite volume fraction decreased. On the other hand, there was no considerable change in microstructure after ageing at 650 °C.
2. DL-EPR results showed by increasing in sensitisation time, DOS increased and as a result the alloy was more susceptible to intergranular corrosion. The specimens aged at 800 °C showed higher value of DOS at all sensitisation times.
3. Potentiostatic CPT measurements revealed by increase in ageing time the CPT value decreased. It can be also reported that ageing at 800 °C has more deteriorative effect on pitting corrosion than 650 °C.
4. A significant decrease in CPT value could be detected in 300 min aged specimen at 800 °C. This decrease in CPT value can be attributed to the change in microstructure of this specimen.
5. In could be realized that the DOS and CPT values show almost a liner relationship at specimens aged at 650 °C, where the microstructure of all specimens showed duplex characteristic. Since by increase in ageing time microstructure changes, this relation could not be observed in the results of 800 °C aged specimens.

Acknowledgements

The authors appreciate the financial support from Ferdowsi University of Mashhad provision of laboratory facilities during the period that this research was conducted and also Mrs. Tolou' Farrokh and Mr. H. Mostajab O Daveh for valuable assistance on microstructure and XRD analysis.

References

[1] B. Deng, Y. Jiang, J. Gong, C. Zhong, J. Gao, J. Li, Critical pitting and repassivation temperatures for duplex stainless steel in chloride solutions, Electrochim. Acta 53 (2008) 5220–5225.
[2] A. Igual Munoz, J. Garcıa Anton, J.L. Guinon, V. Perez Herranz, Inhibition effect of chromate on the passivation and pitting corrosion of a duplex stainless steel in LiBr solutions using electrochemical techniques, Corros. Sci. 49 (2007) 3200–3225.
[3] A. Igual Munoz, J. Garcia Anton, J.L. Guinon, V. Perez Herranz, The effect of chromate in the corrosion behaviour of duplex stainless steel in LiBr solutions, Corros. Sci. 48 (2006) 4127–4151.

[4] A.M. do Nascimento, M.C.F. Ierardi, A.Y. Kina, S.S.M. Tavares, Pitting corrosion resistance of cast duplex stainless steels in 3.5%NaCl solution, Mater. Charact. 59 (2008) 1736–1740.
[5] V.S. Moura, L.D. Lima, J.M. Pardal, A.Y. Kina, R.R.A. Corte, S.S.M. Tavares, Influence of microstructure on the corrosion resistance of the duplex stainless steel UNS S31803, Mater. Charact. 59 (2008) 1127–1132.
[6] V. Muthupandi, P. Bala Srinivasan, S.K. Seshadri, S. Sundaresan, Effect of weld metal chemistry and heat input on the structure and properties of duplex stainless steel welds, Mater. Sci. Eng. A 358 (2003) 9–16.
[7] S.A. Tavara, M.D. Chapetti, J.L. Otegui, C. Manfredi, Influence of nickel on the susceptibility to corrosion fatigue of duplex stainless steel welds, Int. J. Fatigue 23 (2001) 619–626.
[8] I.N. Bastos, S.S.M. Tavares, F. Dalarda, R.P. Nogueira, Effect of microstructure on corrosion behaviour of superduplex stainless steel at critical environment conditions, Scripta Mater. 57 (2007) 913–916.
[9] N. Sathirachinda, R. Pettersson, J. Pan, Depletion effects at phase boundaries in 2205 duplex stainless steel characterised with SKPFM and TEM/EDS, Corros. Sci. 51 (2009) 1850–1860.
[10] M. Pohl, O. Storz, T. Glogowski, Effect of intermetallic precipitations on the properties of duplex stainless steel, Mater. Charact. 58 (2007) 65–71.
[11] R. Hsieh, H. Liou, Y. Pan, Effects of cooling time and alloying elements on the microstructure of the Gleeble simulated heat affected zone of 22%Cr duplex stainless steel, J. Mater. Eng. Perform. 10 (2001) 526–536.
[12] B. Josefsson, J.O. Nilsson, A. Wilson, in: Proceedings Conference ''Duplex Stainless Steels'91'', vol. 2, Beaune, France, 1991, pp. 67–75.
[13] K. Ravindranath, S.N. Malhotra, The influence of ageing on the intergranular corrosion of 22 chromium–5 nickel duplex stainless steel, Corros. Sci. 37 (1995) 121–132.
[14] J. Dobranszky, P.J. Szabo, T. Berecz, V. Hrotko, M. Portko, Energy-dispersive spectroscopy and electron backscatter diffraction analysis of isothermally aged SAF 2507 type superduplex stainless steel, Spectrochim. Acta B59 (2004) 1781–1788.
[15] G.V. Voort, Atlas of Time–Temperature Diagrams for Irons and Steels, ASM International, Materials Park, OH, 1991.
[16] J.O. Nilsson, A. Wilson, Influence of isothermal phase transformation on toughness and pitting corrosion of super duplex stainless steel SAF 2507, Mater. Sci. Technol. 9 (1993) 545–554.
[17] J.O. Nilsson, Overview of super duplex stainless steel, Mater. Sci. Technol. 8 (1992) 685–700.
[18] T.H. Chen, J.R. Yang, Effects of solution treatment and continuous cooling on σ phase precipitation in a 2205 duplex stainless steel, Mater. Sci. Eng. A311 (2001) 28–41.
[19] T.H. Chen, K.L. Weng, J.R. Yang, The effect of high-temperature exposure on the microstructural stability and toughness property in a 2205 duplex stainless steel, Mater. Sci. Eng. A338 (2002) 259–270.
[20] E. Angelini, B.D. Benedetti, F. Rosalbino, Influence of ageing treatment between 700 and 900 °C on localized corrosion resistance of duplex stainless steel SAF2205, Metall. Ital. 88 (1996) 339–344.
[21] E. Angelini, B.D. Benedetti, G. Maizza, F. Rosalbino, Sensitization phenomena on aged SAF 2205 duplex stainless steel and their control by means of EPR tests, Corrosion 55 (1999) 605–615.
[22] L. Duprez, B.D. Cooman, N. Akdut, Microstructure evolution during isothermal annealing of a standard duplex stainless steel type 1.4462, Steel Res. 71 (2000) 417–422.
[23] K.L. Weng, H.R. Chen, J.R. Yang, The low-temperature ageing embrittlement in a 2205 duplex stainless steel, Mater. Sci. Eng. A379 (2004) 119–132.
[24] S.S.M. Tavares, V.F. Terra, J.M. Pardal, M.P.C. Fonseca, Influence of the microstructure on the toughness of a duplex stainless steel UNS S31803, J. Mater. Sci. 40 (2005) 145–154.
[25] S.S.M. Tavares, V.F. Terra, Corrosion resistance evaluation of the UNS S31803 duplex stainless steels aged at low temperatures (350 to 550 °C) using DLEPR tests, J. Mater. Sci. 40 (2005) 4025–4028.
[26] F. Elshawesh, N. Elahresh, A. Elhoud, Effect of r phase on pitting corrosion of 2205 duplex stainless steel, Br. Corros. J. 33 (1998) 285–287.
[27] J.H. Potgieter, Influence of r phase on general and pitting corrosion resistance of SAF 2205 duplex stainless steel, Br. Corros. J. 27 (1992) 219–223.
[28] M. Pohl, O. Storz, Sigma phase in duplex-stainless steels, Z. Metallkd. 95 (2004) 631–638.
[29] C.J. Park, V.S. Rao, H.S. Kwon, Effect of sigma phase on the initiation and propagation of pitting corrosion of duplex stainless steel, Corrosion 61 (2005) 76–83.
[30] N. Lopez, M. Cid, M. Puiggali, Influence of r-phase on mechanical properties and corrosion resistance of duplex stainless steel, Corros. Sci. 41 (1999) 1615–1631.
[31] K.N. Adhe, V. Kain, K. Madangopal, H.S. Gadiyar, Influence of sigma-phase formation on the localized corrosion behaviour of a duplex stainless steel, J. Mater. Eng. Perform. 5 (1996) 500–506.
[32] M.A. Domínguez-Aguilar, R.C. Newman, Detection of deleterious phases in duplex stainless steel by weak galvanostatic polarization in halide solutions, Corros. Sci. 48 (2006) 2577–2591.
[33] ASTM A262 standard practice for detecting the susceptibility to intergranular attach in austenitic stainless steels.
[34] M. Momeni, A. Ale-yassin, M.H. Moayed, A. Davoodi, Development new solution based on $HCl/Na_2S_2O_3$ for detection and measuring stainless steels degree of sensitisation by DL-EPR method, Corros. Sci., submitted for publication.
[35] ISO 17864: Corrosion of metals and alloys—determination of the critical pitting temperature under potentiostatic control, 2005.
[36] B. Deng, Z. Wang, Y. Jiang, T. Sun, J. Xu, J. Li, Effect of thermal cycles on the corrosion and mechanical properties of UNS S31803 duplex stainless steel, Corros. Sci. 51 (2009) 2969–2975.
[37] B.I. Voronenko, Austenitic–ferritic stainless steels: a state of the art review, Met. Sci. Heat Treat. 39 (1997) 20–29.
[38] A. John Sedriks, Corrosion of Stainless Steels, second ed., John Wiley & Sons, Inc., USA, 1996.
[39] B. Deng, Z. Wang, Y. Jiang, T. Sun, J. Xu, J. Li, Evaluation of localized corrosion in duplex stainless steel aged at 850 °C with critical pitting temperature measurement, Electrochim. Acta 54 (2009) 2790–2794.
[40] K. Sugimoto, Y. Sawada, Role of alloyed molybdenum in austenitic stainless steels in the inhibition of pitting in neutral halide solutions, Corrosion 32 (1976) 347–352.
[41] G.T. Burstein, P.C. Pistorius, S.P. Mattin, The nucleation and growth of corrosion pits on stainless steel, Corros. Sci. 35 (1993) 57–62.
[42] L.F.G. Mesias, J.M. Sykes, Metastable pitting in 25Cr duplex stainless steel, Corros. Sci. 41 (1999) 959–987.
[43] M.H. Moayed, R.C. Newman, Evolution of current transients and morphology of metastable and stable pitting on stainless steel near the critical pitting temperature, Corros. Sci. 48 (2006) 1004–1018.
[44] B. Deng, Y.M. Jiang, J.X. Liao, Y.W. Hao, C. Zhong, J. Li, Dependence of critical pitting temperature on the concentration of sulphate ion in chloride containing solutions, Appl. Surf. Sci. 253 (2007) 7369–7375.
[45] M.E. Wilms, V.J. Gadgil, J.M. Krougmen, F.P. Ijsseling, The effect of sigma-phase precipitation at 800 °C on the corrosion resistance in sea-water of a high alloyed duplex stainless steel, Corros. Sci. 36 (1994) 871–881.
[46] R.A. Perren, T. Suter, C. Solenthaler, G. Gullo, P.J. Uggowitzer, H. Böhni, M.O. Speidel, Corrosion resistance of super duplex stainless steels in chloride ion containing environments: investigations by means of a new microelectrochemical method: II. Influence of precipitates, Corros. Sci. 43 (2001) 727–745.